Rapid Communications

Kinetics and structural changes in dynamically compressed bismuth

Charles M. Pépin,[1,*] Arnaud Sollier,[1] Adrien Marizy,[1] Florent Occelli,[1] Mathias Sander,[2] Raffaella Torchio,[2] and Paul Loubeyre[1]

[1]*CEA, DAM, DIF, F-91297 Arpajon, France*

[2]*ESRF, 6 Rue Jules Horowitz, Boîte Postale 220, F-38043 Grenoble Cedex, France*

(Received 5 February 2019; revised manuscript received 24 May 2019; published 5 August 2019)

Synchrotron nanosecond time-resolved x-ray diffraction has been performed on dynamically compressed bismuth along various compression and release paths, hence exploring the Bi phase diagram up to 8 GPa and 600 K. Marked departures from the static phase diagram is observed. The sequence of structural changes is different upon compression and release. The Bi-III complex host-guest structure is never obtained. Instead the Bi-V phase is observed over a large domain. Melting of Bi-V and crystallization of the fluid into Bi-I are clearly identified on stress release. Supercooling and superheating deviations to the equilibrium melting line are observed. These observations on a prototypical system underline the possible deviations between the phase diagram obtained by dynamical compression and the one under static pressure.

DOI: 10.1103/PhysRevB.100.060101

Introduction. The possibility of inspecting the actual atomistic arrangement of a material under dynamical compression is one of the major advances in experimental high pressure over the past decade. It is crucial to obtain an unambiguous understanding of the material's response to dynamical compression and it can now be used to explore the solids structures in the terapascal range [1]. The first x-ray diffraction (XRD) evidence for a phase transition during shock-wave compression was observed in 1972 [2]. Yet, time-resolved x-ray diffraction of dynamically compressed matter could only be obtained recently by using various large x-ray source facilities, such as KJ laser [3,4], x-ray free electron laser [5], and synchrotron [6–8]. Up to now, the differences between dynamic and static data sets have been discussed mostly in terms of the phase transitions kinetics. Observing the structural response of a shocked material now enables rigorous comparisons with the structural phase transitions disclosed by static compression. The long-debated question of a possible large superheating of a solid in the liquid domain can be investigated more accurately. Another interesting question is emerging: Are the dynamically produced structural transformations on a nanosecond compression timescale similar to those observed under static pressure?

In this Rapid Communication, we address this question on bismuth. Bi is an archetypal pressure-induced phase-transforming material showing a complex phase diagram up to 10 GPa, as first revealed by Bridgman [9] and refined by many studies since then [10,11]. As such, the Bi phase diagram is particularly interesting to compare static and dynamic data sets: over a moderate pressure range, it presents a rich structural polymorphism, an unusually complex host-guest structure Bi-III, and a minimum on the melting curve. A few time-resolved XRD studies on shocked Bi have already been published. Hu *et al.* and Gorman *et al.* have recently investigated solid structural transformations, yet with differing conclusions [7,12]. In the first study, the structural sequence observed agreed with the static phase diagram, which reinforces the conclusion on the observation of the thermodynamical equilibrium phase diagram with boundaries shifted by kinetic hindrance. In the second study, the complex Bi-III was not observed upon compression and a metastable phase Bi-M seemed to form instead. Another XRD study investigated superheating of solid Bi at melting, obtaining a 3 ns upper limit for the timescale of melting of Bi under shock loading, a much shorter value than previous estimates obtained by the modeling of wave profiles [5]. In the present study, answers and novel insights have been obtained by following various compression paths and by performing accurate nanosecond time-resolved synchrotron XRD measurements on homogeneous sample states. The Bi-III complex structure is never observed under compression or release dynamical paths. The timescale of melting is determined to be less than 0.5 ns and yet a deviation from equilibrium melting, "superheating," is measured. Besides, a supercooling of the liquid is observed before the crystallization into the Bi-I phase.

Experimental configuration. The measurements were performed on the time-resolved XRD beamline ID09 of the European Synchrotron radiation Facility. The target assembly and the compression schemes were designed to obtain very reproducible single-shot laser-pump/x-ray probe data with a 0.5 ns resolution time delay, to follow different compression paths covering a large domain of the Bi phase diagram below 8 GPa and to perform accurate XRD measurements on homogeneous sample states. As shown in Fig. 5(a) of the Supplemental Material [13], the sample consisted of a 5-μm-thick foil of polycrystalline bismuth (Goodfellow; 99,97% purity) glued to a 100-μm-thick sapphire on the laser side and to a 125-μm-thick polyimide on the other side. The sample assembly was mechanically pressed in the sample holder with a calibrated force to approximately 1 μm in thickness

*charles.pepin@cea.fr

and the epoxy glue layer was then UV cured. Three starting temperatures, 300, 400, and 500 K, of the compression path were studied by preheating the targets with a transportable resistive heater, as described in Ref. [13]. The YAG laser pulse ($\lambda = 1064$ nm) used for compression had a fixed energy of 308 mJ with a Gaussian pulse duration of 5 ns FWHM. The laser was focused at the sapphire/Bi interface with a spot diameter of 250 μm. This confined plasma-driven shock scheme provides an interesting and reproducible pressure time evolution in the Bi sample, as shown in Fig. 5(b) of Ref. [13]. The time $t = 0$ corresponds to the beginning of the Gaussian laser pulse arriving on the Bi sample. Uncertainty in the $t = 0$ timing due to laser jitter is 0.5 ns.

The time evolution of the pressure was measured using the volume of compressed solid obtained from the XRD diffraction pattern and, in the fluid phase, using the peak position of the liquid structure factor [5,14]. The measured pressure evolution is in good agreement with the analytical model of Fabbro *et al.* [15], and with the hydrodynamic simulations using the ESTHER hydrocode [16]. A peak pressure is reached at the end of the laser pulse duration and after the pressure profile decreases with roughly a $2/3$ power law. Such a release is essentially a well-controlled ramp process.

The x-ray pulse used for the XRD was produced by a single bunch current in the synchrotron pulse train and an undulator, giving $\sim 4\times 10^8$ photons monochromatized at 15 keV. The x-ray spot size on the sample was $\sim$60 μm (V) $\times$ 100 μm (H), i.e., significantly smaller than the laser spot size. Further details of the beamline can be found in Ref. [17]. Typical x-ray diffraction patterns measured in the various phases observed on the various compression paths are shown in Fig. 1, namely, Bi-I, Bi-II′, Bi-V, and liquid. Homogeneous Bi states were obtained in contrast to the two previous time-resolved XRD studies [7,12] in which the compressed sample was always constituted of a mixture of phases, indicating a heterogeneous compression of the Bi sample explained by the thicker Bi sample used; respectively, 20 and 8 μm. The XRD pattern quality enables a volume determination and a structure verification with a LeBail refinement. X-ray diffraction measurements were collected with 0.5 ns incremental time delays with respect to the laser initiation. By varying the laser/XRD delay, we were able to probe the structural sample state along the pressure time evolution shown in Fig. 5(b) of Ref. [13]. Along the three compression paths followed, the bismuth sample, initially in the Bi-I rhombohedral structure (space group $R\bar{3}m$, $Z = 2$), always transformed to a Bi-V body-centered cubic (bcc) structure (space group $Im\bar{3}m$, $Z = 2$). As discussed below, other structural changes were observed upon pressure release. Three Bragg peaks of the bcc Bi-V structure could clearly be observed, enabling one to accurately determine the volume. The pressure is then obtained using the very-well established equation of state of Bi-V [14] (and of Bi-I upon release [10]). Error bars on the pressure originate from the pressure gradient in the sample of $\sim$0.2 GPa and from the propagation of the uncertainty on the temperature ($\pm$35 K) through a linear thermal expansion [18]. The temperature uncertainty comes from the uncertainty in the initial temperature at the target center, $\pm$5 K, and from the difference between the true compression path from hydrodynamic simulations and the estimation of temperature assuming a

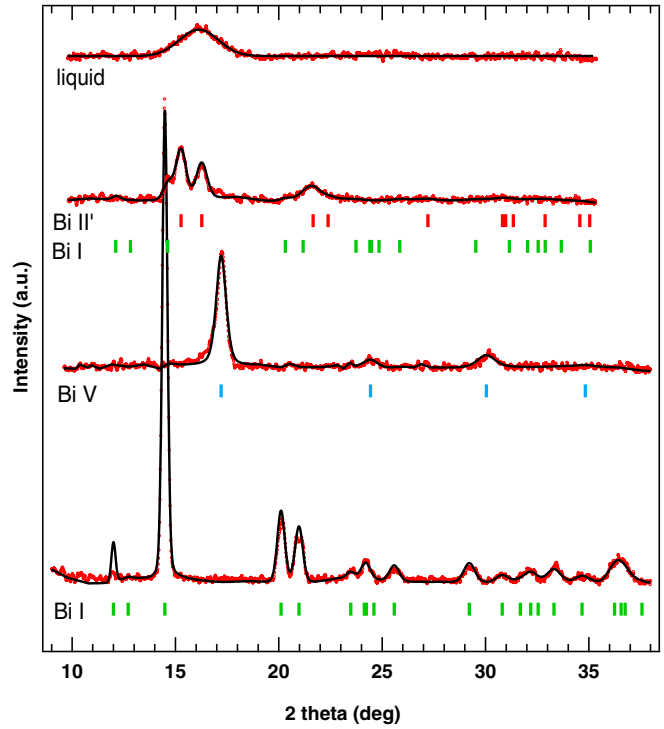

FIG. 1. Integrated x-ray diffraction patterns (red points) with a LeBail refinement (black lines) for Bi-I, Bi-V, and Bi-II′, taken at $\lambda = 0.8266$ Å. The diffuse scattering peak of the liquid is also shown. Colored ticks correspond to the theoretical positions of the Bragg peaks for Bi-I (green), Bi-V (blue), and Bi-II′ (red).

Hugoniot compression or an isentrope release. Using ESTHER hydrocode simulations, this difference in temperature is estimated to $\pm$30 K. Finally, upon the melting of Bi-V, there should be a discontinuity of temperature on the release path that is estimated experimentally by following the solid/fluid equilibrium along the melting line over few incremental XRD times (see Fig. 8 of Ref. [13]). At the fluid crystallization into Bi-I, an inverse temperature discontinuity is assumed. The pressure in the fluid phase was estimated from the main peak structure factor position, for which a linear shift versus pressure was previously calibrated based on shock, diamond anvil cell, and large volume press data [5].

Solid structural transformations. The compression path obtained by dynamically compressing the Bi target at 300 K was aimed at probing structural differences in the solid phases when compared to static pressure results. In the dynamic compression configuration used, with a fixed laser energy, the initial pressure obtained was around 4 GPa [see Fig. 5(b) of Ref. [13]]. As shown in Fig. 2, the compression path over time should cross various phase boundary lines of the static phase diagram and so should give the following sequence of phases: Bi-I, Bi-II, Bi-III, and Bi-V upon compression and reversely upon release. Initially, the bismuth sample target is in the rhombohedral phase Bi-I. Bi-I is observed to transform into Bi-V for pressures as low as $\sim$4.3 GPa. The XRD data obtained slightly below indicate deviation from a pure Bi-V structural pattern, by presenting extra peaks. The main evidence is a shoulder on the main Bragg peak of Bi-V located at 16.75°, as shown in Fig. 9 of Ref. [13]. That is in good

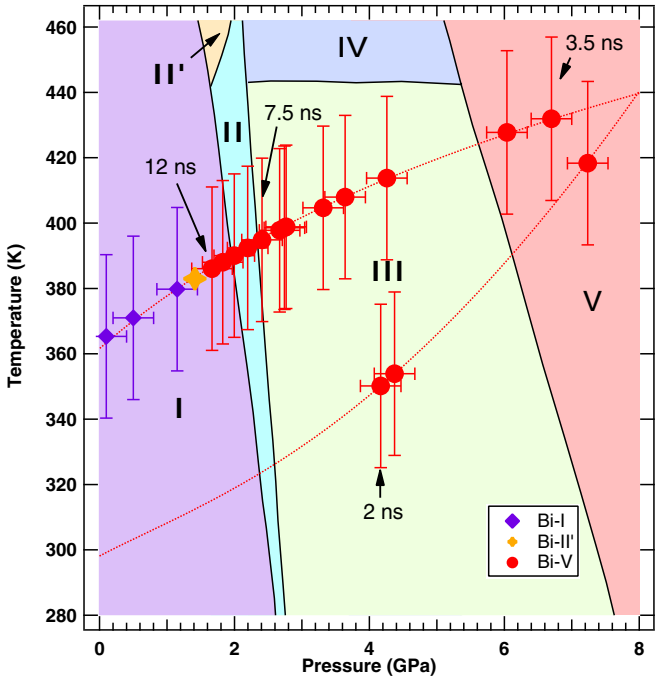

FIG. 2. Compression and release path for the starting temperature of 300 K is shown superimposed to the known phase diagram of Bi. The Bi-II and Bi-III phases expected from the previous static measurements are never observed during the release; instead Bi-II′ appears at longer delays.

agreement with a recent time-resolved XRD study [12] presenting a similar diffraction pattern over the pressure region 3–4 GPa, which was explained by the formation of an intermediate structure, Bi-M. In this previous time-resolved diffraction study, by probing shocked states below 4 GPa, the sequence Bi-I, Bi-II, Bi-*M*, and Bi-V was obtained. We confirm here the existence of Bi-*M*, the nonformation of Bi-III, and instead the formation of Bi-V at lower pressure than its stability domain observed under static compression. On the other hand, the structural transformation on the release compression path is very different from what was reported previously [7]. Here, the sequence Bi-V, Bi-II′, and Bi-I is observed, whereas previously the Bi-V,Bi-III,Bi-II,Bi-I sequence was reported. The reason for this discrepancy is probably a wrong interpretation of the structural pattern due to the poor structural data quality and the heterogeneous state of the sample, whereas in the present study an unambiguous Lebail fit of the structural data of a homogeneous state has been made. Bi-II′ is a metastable tetragonal polymorph of Bi observed in a small region below the melting line [19]. The novel result obtained here is that the Bi-III complex host-guest structure is observed neither under compression nor under dynamical loading release, with respective compression times of 2 and 10 ns.

Under static pressure conditions, the existence of Bi-III has been interpreted as an intermediate structural path to achieve the reconstructive transformation from Bi-I to Bi-V. Above 200 K, the transformation of Bi-I to Bi-III is, however, not direct, with an intermediate structural transformation to Bi-II, existing over a narrow pressure stability range. Some characteristics of this structural sequence highlight the fact that the Bi-V to Bi-III phase transition should be easier than the Bi-I to Bi-III one. The Bi-I to Bi-III transition mechanism is reconstructive, whereas a displacive mechanism is associated with the Bi-III to Bi-V phase transition [20]. The Bi-I to Bi-V transition is associated to a strong increase of the effective coordination number from 6 to 11 and to a large volume discontinuity. The effective coordination number in Bi-III is intermediate, around 8, but the volume discontinuity from Bi-I to Bi-III of $\Delta V/V \sim 8\%$ is much larger than the Bi-III to Bi-V one of $\Delta V/V \sim 1.3\%$ [10]. *Ab initio* calculations have also shown that the difference of enthalpy between Bi-III and Bi-V is small; less than 0.03 eV/atom [21].

Current knowledge on the structural changes expected under dynamical compression is that the equilibrium structural transformation sequence should be preserved, yet with transition lines shifted in pressure due to kinetic hindrance [22]. It is based on the fact that the incubation period, related to the formation of the new phase, should decrease logarithmically with the deviation ΔP from the equilibrium transition line. For a large enough ΔP, the incubation time should become compatible with the timescale of the compression. Because Bi-III is a complex incommensurate host-guest structure, its nucleation time could be long and therefore the ΔP needed for reducing its incubation time to the few nanoseconds value could be larger than the ∼3 GPa extent of Bi-III equilibrium stability domain. Indeed, a very similar incommensurate host-guest structure has been observed in shock-compressed scandium with a ΔP around 25 GPa [23]. But that cannot explain why on compression Bi-V is observed at lower pressure than its equilibrium stability domain; Bi-II should have been observed instead. Besides, on the release path, the Bi-V to Bi-III transformation, being less kinetically hindered due to the displacive mechanism relating these two structures, should have been observed. So, another explanation might be operative here: the shear stress component existing under shock compression could stabilize Bi-V over Bi-III, all the more so as the enthalpies of both phases are very near. Unfortunately, the quality of the XRD data is not good enough here to estimate the existing deviatoric stress on shocked Bi, as done in DAC static synchrotron measurements [24]. It was recently shown that by changing the stress conditions in a DAC experiment, a metastable Bi-liquid phase could be stabilized [25]. A static high pressure experiment with controlled deviatoric stress should now be designed to validate possible stabilization of Bi-V by nonhydrostatic pressure components to confirm this interpretation.

Melting. Superheating and undercooling are inherent in the melting and freezing processes. Superheating and undercooling temperatures should be of similar amount in the framework of homogeneous nucleation theory and should increase with the rate of crossing the melting line (varying T, P, or both). Yet, superheating is generally drastically reduced due to heterogeneous nucleation. Thereof, the question of bulk superheating of solids under dynamical compression has long been debated. In the case of Fe [26], the good agreement between static and dynamic compression has recently suggested that superheating was not detrimental for the determination of the melting line using shock compression. The question of superheating has also continuously been investigated in Bi, using advances in the experimental techniques to reach

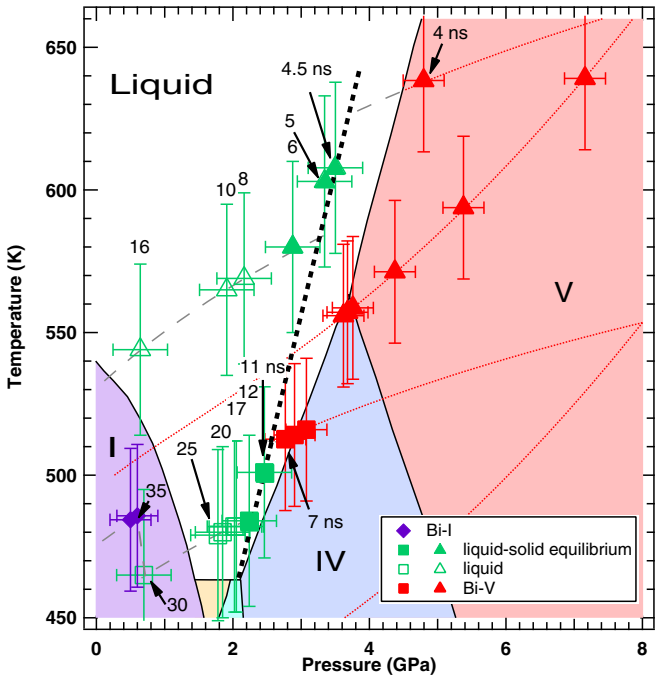

FIG. 3. Compression and release paths for the starting temperatures of 400 and 500 K. A superheating of ∼60 K is observed during the release when going from Bi-V to the liquid phase. An undercooling of ∼80 K is measured when transforming from the liquid to the solid Bi-I phase.

a more rigorous answer [5,27,28]. Superheating by about 90 K has been reported in single crystal Bi-I under a heating rate of $\sim 10^{11}$ K/s [28]. Release from shock pressure using time-resolved XRD, i.e., comparable to the present experiment, has shown that the liquid state is found in less than 3 ns, from which no evidence of superheating of Bi-V in the liquid was inferred within the accuracy of the *P-T* estimate. Here, by preheating the Bi target to 400 and 500 K, the release curve is crossing the Bi-V melting line at two points, as shown in Fig. 3. The bulk melting of the sample is clearly identified on the XRD pattern by going from the Bi-V diffraction peaks to the liquid diffuse scattering ring (see Fig. 1). The melting process occurs in less than 0.5 ns, the incremental time delay of our data acquisition. The fraction of solid compared to liquid then decreases with the release path following the melting line over 1 ns. It should be noted that Bi-V is observed until melting along the 400 K release path, although in the static phase diagram Bi-IV should be the stable phase. However, there is no discontinuity on the equilibrium melting line by going from the Bi-IV to the Bi-V phase.

The inferred melting line, as determined here by the two data points obtained on the two release paths, is seen shifted from the equilibrium one. This shift corresponds to a superheating of about 60 K, which is in good agreement with the measured superheating of Bi-I (the effective cooling rate here is similar to the heating rate used for superheating Bi-I [28]). The 400 K target release path also crosses the melting line of Bi-I but at longer delays. The crystallization of the fluid into Bi-I is observed in the XRD pattern with a change from the one peak structure factor to diffraction peaks of phase I. This recrystallization is also strong evidence that the diffuse scattering diffraction signal originates from a liquid rather than from an amorphous state. Because the time step was 5 ns at the end of the release path, the nucleation time for the solid is estimated in between 5 and 10 ns. A significant undercooling of the fluid is observed; about 80 K compared to the equilibrium melting line. This undercooling temperature is almost identical to the superheating temperature of the single crystal of Bi-I, in agreement with the homogeneous nucleation model for the solid-fluid transition; not so surprising though since the heterogeneous nucleation contributions due to defects were reduced by heating a single crystal [28].

Conclusion. At intermediate strain rates, using a dynamic diamond-anvil cell [29], no deviation from the static phase diagram is observed. We show here that at higher strain rates, the phase diagram measured under nanosecond compression experiment can be very different from the one measured in static experiments, not only, as well known, by shifting the boundary lines between various phases but more surprisingly by giving a different sequence of structures. It is an important fact to consider when analyzing structural changes under ramp compression, which is now a very promising approach to explore the phase diagram of materials in the terapascal pressure range. Considering that static high-pressure experiments using new diamond-anvil cell designs [30,31] are now well on their way to this pressure range, the comparison of static and dynamic should help to explore structures stabilized by strain rates or deviatoric stress.

Acknowledgments. The authors thank L. Videau for his comments and help with ESTHER. The authors aknowledge the European Synchrotron Radiation Facility for provision of synchrotron radiation on beamline ID09 (proposal HC3971).

[1] J. R. Rygg, J. H. Eggert, A. E. Lazicki, F. Coppari, J. A. Hawreliak, D. G. Hicks, R. F. Smith, C. M. Sorce, T. M. Uphaus, B. Yaakobi, and G. W. Collins, Rev. Sci. Instrum. **83**, 113904 (2012).

[2] Q. Johnson and A. C. Mitchell, Phys. Rev. Lett. **29**, 1369 (1972).

[3] R. W. Lee, M. J. Eckart, J. D. Kilkenny, R. R. Whitlock, A. Hauer, and J. S. Wark, Short pulse x-ray diffraction studies of shocked and annealed crystals using the Janus research laser, in *Proceedings of the 31st Annual Technical Symposium on Optical and Optoelectronic Applied Sciences and Engineering, San Diego, CA, 17–21 Aug. 1987*, edited by Martin C. Richardson, X-Rays from Laser Plasmas Vol. 0831 (SPIE, 1988).

[4] D. H. Kalantar, J. F. Belak, G. W. Collins, J. D. Colvin, H. M. Davies, J. H. Eggert, T. C. Germann, J. Hawreliak, B. L. Holian, K. Kadau, P. S. Lomdahl, H. E. Lorenzana, M. A. Meyers, K. Rosolankova, M. S. Schneider, J. Sheppard, J. S. Stolken, and J. S. Wark, Phys. Rev. Lett. **95**, 075502 (2005).

[5] M. G. Gorman, R. Briggs, E. E. McBride, A. Higginbotham, B. Arnold, J. H. Eggert, D. E. Fratanduono, E. Galtier, A. E. Lazicki, H. J. Lee *et al.*, Phys. Rev. Lett. **115**, 095701 (2015).

[6] S. J. Turneaure, N. Sinclair, and Y. M. Gupta, Phys. Rev. Lett. **117**, 045502 (2016).
[7] J. Hu, K. Ichiyanagi, T. Doki, A. Goto, T. Eda, K. Norimatsu, S. Harada, D. Horiuchi, Y. Kabasawa, S. Hayashi *et al.*, Appl. Phys. Lett. **103**, 161904 (2013).
[8] R. Briggs, R. Torchio, A. Sollier, F. Occelli, L. Videau, N. Kretzschmar, and M. Wulff, J. Synchrotron Rad. **26**, 96 (2019).
[9] P. W. Bridgman, Phys. Rev. **60**, 351 (1941).
[10] M. I. McMahon, O. Degtyareva, and R. J. Nelmes, Phys. Rev. Lett. **85**, 4896 (2000).
[11] S. Ono, High Press. Res. **38**, 414 (2018).
[12] M. G. Gorman, A. L. Coleman, R. Briggs, R. S. McWilliams, D. McGonegle, C. A. Bolme, A. E. Gleason, E. Galtier, H. J. Lee, E. Granadosand *et al.*, Sci. Rep. **8**, 16927 (2018).
[13] See Supplemental Material at http://link.aps.org/supplemental/10.1103/PhysRevB.100.060101 for a description of the resistive heater used for high temperature runs, of the Fabbro model and of the ESTHER hydrosimulation. It also contains a description of the target and of the pressure determination in the solid and in the liquid.
[14] Y. Akahama and H. Kawamura, J. Appl. Phys. **92**, 5892 (2002).
[15] R. Fabbro, J. Fournier, P. Ballard, D. Devaux, and J. Virmont, J. Appl. Phys. **68**, 775 (1998).
[16] J. P. Colombier, P. Combis, F. Bonneau, R. LeHarzic, and E. Audouard, Phys. Rev. B **71**, 165406 (2005).
[17] M. Wulff, A. Plech, L. Eybert, R. Randler, F. Schotte, and P. Anfinrud, Faraday Discuss. **122**, 13 (2003).
[18] G. V. Samsonov, *Handbook of the Physicochemical Properties of the Elements* (IFI Plenum, New York - Washingthon, 1968).
[19] E. Principi, M. Minicucci, A. Di Cicco, A. Trapananti, S. De Panfilis, and R. Poloni, Phys. Rev. B **74**, 064101 (2006).
[20] H. Katzke and P. Tolédano, Phys. Rev. B **77**, 024109 (2008).
[21] U. Häussermann, K. Söderberg, and R. Norrestam, J. Am. Chem. Soc. **124**, 15359 (2002).
[22] R. F. Smith, J. H. Eggert, M. D. Saculla, A. F. Jankowski, M. Bastea, D. G. Hicks, and G. W. Collins, Phys. Rev. Lett. **101**, 065701 (2008).
[23] R. Briggs, M. G. Gorman, A. L. Coleman, R. S. McWilliams, E. E. McBride, D. McGonegle, J. S. Wark, L. Peacock, S. Rothman, S. G. Macleod *et al.*, Phys. Rev. Lett. **118**, 025501 (2017).
[24] K. Takemura and A. Dewaele, Phys. Rev. B **78**, 104119 (2008).
[25] C. Lin, J. S. Smith, S. V. Sinogeikin, Y. Kono, C. Park, C. Kenney-Benson, and G. Shen, Nat. Commun. **8**, 14260 (2017).
[26] S. Anzellini, A. Dewaele, M. Mezouar, P. Loubeyre, and G. Morard, Science **340**, 464 (2013).
[27] J. R. Asay, J. Appl. Phys. **45**, 4441 (1974).
[28] E. A. Murphy, H. E. Elsayed-Ali, and J. W. Herman, Phys. Rev. B **48**, 4921 (1993).
[29] Z. Jenei, H. P. Liermann, R. Husband, A. S. J. Méndez, D. Pennicard, H. Marquardt, E. F. O'Bannon, A. Pakhomova, Z. Konopkova, K. Glazyrin *et al.* , Rev. Sci. Instrum. **90**, 065114 (2019).
[30] L. Dubrovinsky, N. Dubrovinskaia, V. B. Prakapenka, and A. M. Abakumov, Nat. Commun. **3**, 1163 (2012).
[31] A. Dewale, P. Loubeyre, F. Occelli, O. Marie, and M. Mezouar, Nat. Commun. **9**, 2913 (2018).